REGULAR ARTICLE

Otolith morphogenesis during the early life stages of fish is temperature-dependent: Validation by experimental approach applied to European seabass (*Dicentrarchus labrax*)

Kélig Mahé[1] | Frédéric Clota[2] | Marie Odile Blanc[3] | Geoffrey Bled Defruit[1] |
Béatrice Chatain[3] | Hélène de Pontual[4] | Rachid Amara[5] | Bruno Ernande[3,6]

[1]IFREMER, Unit HMMN, Laboratoire ressources halieutiques, Boulogne-sur-mer, France

[2]INRA, Unit 0558, Department PHASE, Nouzilly, France

[3]MARBEC, Université Montpellier, Ifremer, CNRS, IRD, Montpellier, France

[4]IFREMER, Centre de Bretagne, Sciences et Technologies Halieutiques, Plouzané, France

[5]Université Littoral Côte d'Opale, UMR 8187, LOG, Laboratoire d'Océanologie et de Géosciences, Wimereux, France

[6]Evolution and Ecology Program, International Institute for Applied Systems Analysis, Laxenburg, Austria

Correspondence
Kélig Mahé, IFREMER, Unit HMMN, Laboratoire ressources halieutiques, Boulogne-sur-mer, France.
Email: kelig.mahe@ifremer.fr

Abstract

Otolith shape is often used as a tool in fish stock identification. The goal of this study was to experimentally assess the influence of changing temperature and ontogenic evolution on the shape component of the European seabass (*Dicentrarchus labrax*) otolith during early-life stages. A total of 1079 individuals were reared in a water temperature of 16°C up to 232 days post hatch (dph). During this experiment, several specimens were transferred into tanks with a water temperature of 21°C to obtain at the end of this study four different temperature treatments, each with varying ratios between the number of days at 16 and 21°C. To evaluate the otolith morphogenesis, samples were examined at 43, 72, 86 and 100 dph. The evolution of normalized otolith shape from hatching up to 100 dph showed that there were two main successive changes. First, faster growth in the antero-posterior axis than in the dorso-ventral axis changed the circular-shaped otolith from that observed at hatching and, second, increasing the complexity relating to the area between the rostrum and the anti-rostrum. To test the effect of changing temperature, growing degree-day was used in three linear mixed-effect models. Otolith morphogenesis was positively correlated to growing degree-day, but was also dependent on temperature level. Otolith shape is influenced by environmental factors, particularly temperature, making it an efficient tool for fish stock identification.

KEYWORDS
directional asymmetry, growing degree-day, multivariate mixed-effects models, ontogenic effect, otolith shape

1 | INTRODUCTION

The identification of drivers of fish growth is necessary for ongoing sustainable management of commercial species. Fish growth is determined essentially by genetic variation and the phenotypic plasticity, which is an adaptive physical response (e.g., changes of morphometrics, behavior, physiology, metabolism) of a specific genotype to environmental conditions (Fusco & Minelli, 2010; Price et al., 2003). Among environmental factors (e.g., salinity, oxygen, available food, pH, chlorophyll-a, currents, depth, light, etc.), water temperature is the
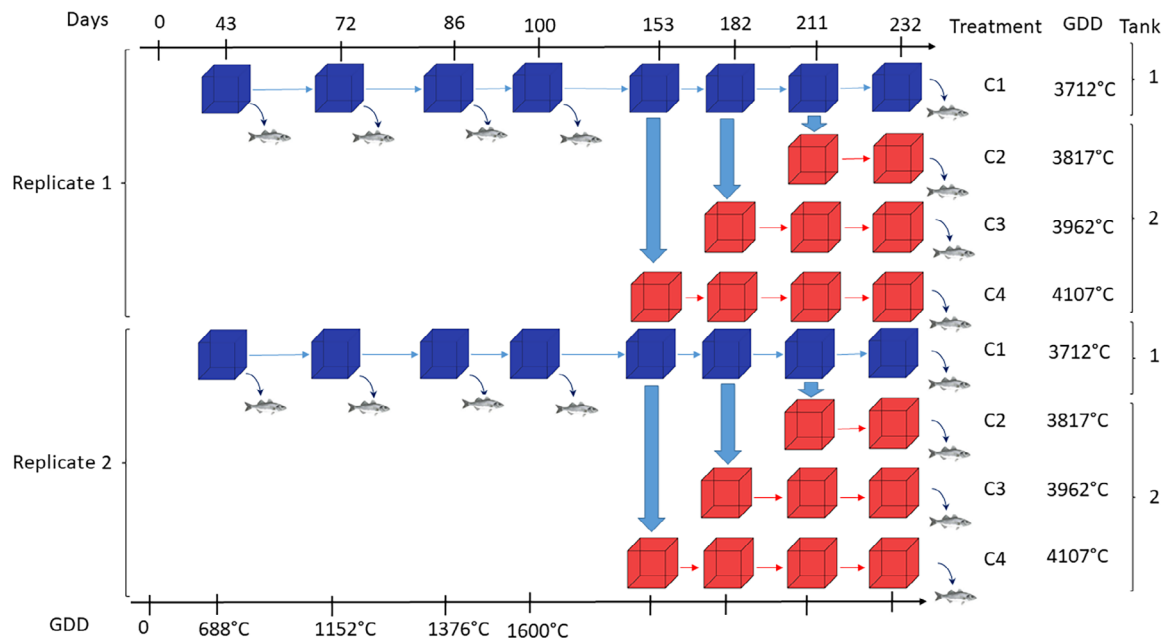
FIGURE 1 Main steps in the experimental design for seabass with four samplings at 43 dph (growing degree-day [GDD] = 688°C · day), 72 dph (GDD = 1152°C · day), 86 dph (GDD = 1376°C · day), and 100 dph (GDD = 1600°C · day). At the end (232 dph), there were four treatments with different GDD values according the transfer date from 16°C (blue) to 21°C (red) (153 dph = 4107°C · day, 182 dph = 3962°C · day, 211 dph = 3817°C · day, and 232dph = 3712°C · day). For each sampling date and condition, there were two replicates (curved arrows and fish icons indicated the sampling fish; wide blues arrows indicated transfer of fish).

most important factor that influences fish growth. The temperature effect on the growth of fish is well known, from the beginning of the 20th century especially (Fulton, 2004). Ocean temperature, within the optimum thermal ranges of species, can increase growth rates as fish are ectothermic (Barrow et al., 2017; Neuheimer et al., 2011; Smoliński & Mirny, 2017). In fact, the very common model of Von Bertalanffy was based on the correlation between the oxygen consumption of fish and the rate of protein degradation determined by the temperature effect to model the growth of fish (Brett, 1979). Moreover, this environmental factor in particular is changing in response to global climate evolution, with the ocean forecast to warm by up to 5°C by 2100 and increasing occurrences of extreme climatic events (IPCC, 2014). Several studies have shown that elevated temperatures may significantly influence whole ecosystems and/or affect the physiology of animals (specifically above organisms' thermal optima or tolerance) (Hay et al., 2005; Hofmann & Todgham, 2010; Mieszkowska et al., 2006; Pörtner & Knust, 2007; Thomas et al., 2004).

The otoliths, calcified structures, which are metabolically inert and located in the inner ear cavity, grow during the life of the fish and retain chemical and physical signatures that correspond to biological and environmental histories throughout a fish's life (Casselman, 1983), therefore a direct proportionality exists between otolith growth and fish growth (Fossen et al., 2003; Lagardère & Troadec, 1997; Mahé et al., 2017). The otolith shape within species can be used to identify and then discriminate stock-units because it integrates variability in environmental conditions and climate forcing that affect life-history characteristics and the genetic

differentiation. Otolith shape differences have been attributed to regional differences in fish metabolic activity due to environmental factors and genetic contribution, which alter the growth of otoliths, determining the size and shape of individual otoliths (Begg & Brown, 2000; Gauldie & Nelson, 1990; Smith, 1992). Since 1993, many fishery scientists have developed this type of analysis for stock discrimination studies. The otolith morphogenesis was characterized from originally being circular at the larval stage, to a more complex shape for the adult stage, described in gadoid species studies as elongation due to the rise in the number of lobes and in flatfish as a progressing number of secondary growth centers (Brown et al., 2001; Irgens et al., 2017; Jearld Jr. et al., 1993; Lagardère & Troadec, 1997; Modin et al., 1996). This development of otolith shape is influenced by environmental factors (Hüssy, 2008; Irgens et al., 2017), with possible varying differences between the right and left inner ear that provide directional asymmetry on otolith shape (Mahé et al., 2018; Mille et al., 2015). During the first life stages (larvae and juveniles), the small size of otoliths and their fast relative accretion rates could result in a better detection of the potential effect of genetic or environmental drivers than during the adult stage. This experimental study examined the otoliths of fish from hatching to 232 days post hatch (dph) (Figure 1). The studied species, European seabass (*Dicentrarchus labrax*, L. 1758), is a commercially important species in Europe and represents a key organism in experimental studies. Finally, contrary to gadoid or flatfish species, the structure of the otolith outline of this species shows no lobes and no secondary

growth centers. Consequently, this study investigated two primary questions:

How does the otolith shape differ according to the ontogenic development from the circular shape?

How does changing temperature affect the otolith shape and size parameters?

While the temperature effect has already been studied from experimental designs using parallel monitoring at different temperatures, the effect of temperature change at several times during the experiment has been little studied. Consequently, to determine the answer to these crucial questions in this paper, elliptic Fourier analysis, size parameter and shape indices, combined with mixed-effects models were used to distinguish differences in otolith shape resulting from the experimental treatments. Otolith information combined with mixed-effects modeling provides a powerful approach for estimating biological (intrinsic) and environmental (extrinsic) effects (Mahé et al., 2019; Martino et al., 2019; Morrongiello & Thresher, 2015; Weisberg et al., 2010).

2 | MATERIALS AND METHODS

2.1 | Ethics Statement

All experimental protocols used to handle the fish were realized at the IFREMER Institute and approved by the French Animal Care and Use Committee (N° Autor.APAFIS#9046). All methods were carried out in accordance with relevant guidelines and regulations.

2.2 | Experimental design

This study was carried out on 1079 European sea bass produced in March 2017 by artificial fertilization in a full factorial mating from a West Mediterranean population. Floating eggs were separated from sinking (dead) ones 48 hours post spawn (2 dph) according to the sea bass rearing standard (by decantation at a salinity of 38‰) and introduced in equal proportion into two 450-L tanks with a water temperature of 16°C. Juvenile European sea bass were hatched and reared at the Ifremer aquaculture experimental research station in Palavas-les-Flots (Hérault, France). Four samplings were made at 43, 72, 86 and 100 dph (the first sampling after 6 life weeks and then the three other samplings taken every 2 weeks; Figure 1 and Table S1). At 100 dph, all fish had reached the minimum size to be tagged with a nanotag (size 1 × 6 mm, mass 10 mg, frequency 13.56 MHz; Lutronics, Nonatec RFID, Lutronic International, www.nonatec.net) according to the standard tagging procedure (Ferrari et al., 2014) and all transferred fish from one replicate at 16°C were reared in one replicate at 21°C. These two temperature conditions were selected because 16°C is the value for the natural conditions and 21°C is the experts' prediction according to the global warming scenario (IPCC, 2014). Throughout the experiment, fish density remained comparable among all tanks. During the study period, no cannibalism was noted. Moreover, no difference in food availability between large and

small individuals was observed. After 100 dph, several specimens (Table S1) from two 450-L tanks with water temperature 16°C were transferred at 153, 182 and 211 dph to two 450-L tanks with water temperature 21°C to obtain at the end of this study (232 dph) resulting in 4 temperature treatments with the different ratios between the days number at 16 and 21°C (Figure 1). All sampled fish were measured (total length [TL] ±0.1 mm) from digitized images using the image-analysis software TNPC (Digital processing for calcified structures, version 7). This process uses an automatic procedure to extract TL information from calibrated images. To analyze the temperature effect on the growth of fish or otoliths, we used the thermal time or Heat Units, a concept that has been widely used to determine this since 1735 (Réaumur, 1735) for the effect of growing season length on vegetables and field crops (Bonhomme, 2000; Trudgill et al., 2005), which is based on the growing degree-days (GDD) (Neuheimer & Taggart, 2007) as follows:

$$GDD = \sum_{i=1}^{n} (Ti - Tth) * \Delta d \qquad (1)$$

where Ti represents the daytime temperature at i, Tth is the threshold temperature, and Δd is the time. In this case, Tth was set at 0°C because the effect of threshold temperature included in the GDD formula had no significant effect on the results of the models. This degree-day approach quantifies the thermal opportunity for growth by aggregating temperatures relevant to growth, and consequently integrates the temperature variation along the life and the exposition time for each temperature, unlike the classic calendar time approach (Legg et al., 1998). Consequently, four temperature treatments with different ratios between the days number at 16 and 21°C, sampled at end of this study showed different values of GDD according to the day of transfer (Figure 1).

2.3 | Otolith shape analysis and measures

Sagittal otoliths (left and right otoliths) were extracted from the cranial cavity. After cleaning, to minimize distortion errors within the normalization process during image analysis, each otolith was placed on a microscope slide with the sulcus facing downward and the rostrum pointing left. The outlines of the otoliths were digitized using an image analysis system consisting of a high-resolution camera connected to an automated microscope using reflected light. Each digitized image was analyzed as fish shape using the image-analysis software TNPC (Digital processing for calcified structures, version 7). To compare the shapes of left and right otoliths, a mirror image of the right otolith was used. Otolith shape was assessed using three methods: size parameters (length, OL; width, OW; perimeter, PO; area, OA), shape indices (form-factor, OFF; roundness, ORD; circularity, OCI; ellipticity, OEL; aspect-ratio, OAR; rectangularity, ORE), and elliptic Fourier descriptors (EFDs) (Lestrel, 2008) (Table S2). These indices described specific aspects of shape as surface area irregularity, circle shape, ellipse shape, and rectangularity shape. All EFDs were obtained using R software from image binearization. For each otolith, the first 99 elliptical Fourier harmonics

(H; each harmonic has four EFDs) were extracted and automatically normalized with respect to the first harmonic (Harmonic 1) and were thus invariant to otolith size, rotation, and the starting point of the contour description (Kuhl & Giardina, 1982). To determine the number of harmonics required to reconstruct the otolith outline, the cumulated Fourier power (F) was calculated for each individual otolith as a measure of the precision of contour reconstruction obtained with the harmonics (i.e., the proportion of variance in contour coordinates accounted for by the harmonics):

$$F_{(n_k)} = \sum_{i=1}^{n_k} \frac{A_i^2 + B_i^2 + C_i^2 + D_i^2}{2} \qquad (2)$$

where A_i, B_i, C_i, and D_i are the coefficients of the harmonic. $F(n_k)$ and n_k were calculated for each individual otolith to ensure that each individual otolith in the sample was reconstructed with a precision of 99.99% (Lestrel, 2008). The maximum number of harmonics across all otoliths was then used to reconstruct each individual otolith. To test the EFDs of the otolith outline, principal components analysis (PCA) was applied to the EFD matrix and a subset of the resulting principal components (PCs) was then selected as otolith shape descriptors according to the broken stick model (Legendre & Legendre, 1998). This procedure allowed us to reduce the number of variables used to describe otolith shape variability while ensuring that the main sources of shape variation were kept, as well as to avoid colinearity between shape descriptors.

2.4 | Statistical analyses

2.4.1 | Directional asymmetry

All descriptors of otolith shape (size parameters, shape indices, and EFDs) were tested to analyze the directional asymmetry between left and right otolith shape (i.e., the effect of inner ear location or side on otolith shape, Si) using linear mixed-effects models (univariate models for size parameters and shape indices, and multivariate models for shape matrix S):

$$O \sim \alpha_0 + \Delta\alpha_{0,in} + \alpha_1 Si + \alpha_2 GDD + \alpha_3 Si * GDD \qquad (3)$$

where inner ear side (Si) and growing degree day (GDD) are fixed effects and individual (in) is introduced as a random effect ($\Delta\alpha_{0,in}$) on the intercept to account for the fact that left and right otolith shapes are more likely to be similar when they originate from the same individual. The multivariate versions of equation (3) applied to shape matrix S were fitted while accounting for variance heterogeneity between PCs (columns of S). The normality of the residuals and the random effects as well as homoscedasticity of the residuals were assessed by visual inspection of diagnostic plots. The models were fitted by maximizing the restricted log-likelihood. The significance of the fixed effects was tested by likelihood ratio tests between nested models while respecting the marginality of the effects (type 2 tests; Legendre & Legendre, 1998), which are supposed to follow a χ^2 distribution under the null hypothesis. The p values were adjusted for multiple comparisons through the Bonferroni correction (McDonald, 2014). To visualize differences in otolith shape between the right and left sides, an average otolith shape of each side group was rebuilt based on the EFDs of the averaged shape, and the percentage of nonoverlapping surface between the right and left otolith mean shapes was calculated.

2.4.2 | Temperature effect on the otolith shape

To test the temperature (T) effect on the otolith shape (O, described by size parameters, or shape indices or the PCs matrix for EFDs) between the four temperature treatments, three mixed-effects models (multivariate for EFDs and univariate for size parameters or shape indices) were fitted and compared:

$$O \sim \alpha_0 + \alpha_1 * GDD \qquad (4)$$

$$O \sim (\alpha_0 + \mu_{0,C}) + \alpha_1 * GDD \qquad (5)$$

$$O \sim (\alpha_0 + \mu_{0,R} + \mu_{0,C}) + (\alpha_1 + \mu_{1,R}) * GDD \qquad (6)$$

where otolith shape variations due to GDD are represented by fixed effects. Random effects (i) were used to account for variability due to rearing tanks/replicates ($\mu_{0,R}$) and also if there was an effect of temperature other than GDD ($\mu_{0,C}$). These models were fitted with a modeled different variance heterogeneity for each PC of the shape matrix S. The three models were fitted by maximizing the restricted log-likelihood. We tested the probability ($p < 0.05$) between all models to choose the most appropriate model. Finally, the significance of GDD at 5% was tested by likelihood ratio tests between nested models while respecting the marginality of the effects (type 2 tests) that are supposed to follow a χ^2 distribution under the null hypothesis. As for side effect analysis, to visualize and to evaluate the amplitude difference differences in otolith shape between groups characterized by different treatments, an average otolith shape by group was rebuilt based on the EFDs of the averaged shape and the percentage of nonoverlapping surface between two groups was calculated. Finally, the significance of shape difference between all group pairs was tested using a mixed-effects model while correcting for multiple comparisons using a Bonferroni procedure. Statistical analyses were performed using the following packages in the statistical environment R: "nlme" (Pinheiro et al., 2016), "lme4" (Bates et al., 2011), "ggplot2" (Wickham, 2016), "gridExtra" (Auguie & Antonov, 2017), "car" (Fox & Weisberg, 2011), and "MASS" (Venables & Ripley, 2002).

3 | RESULTS

3.1 | Ontogenic effect

To analyze the EFDs of the otolith outline, the first 99 Fourier harmonics were extracted from each individual otolith's contours. Only the first 32 harmonics were necessary to explain 99.99% of the
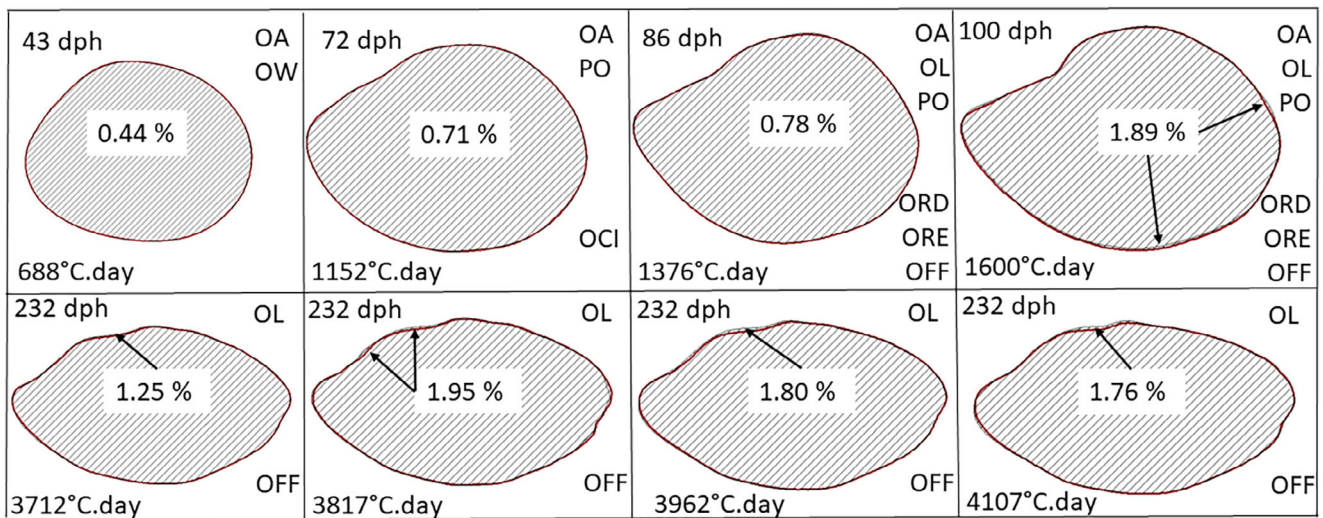
FIGURE 2 Percentage of nonoverlapping surface between left (red line) and right (black line) otolith shapes according to the sampling date (dph) and growing degree-day (GDD) value (°C · day) (arrows indicate the main areas of difference between the otoliths). The size dimension parameters and shape indices of the otolith used to describe seabass otolith outline are identified according to the sampling date and the GDD value when the difference between side was significant ($p < 0.05$).
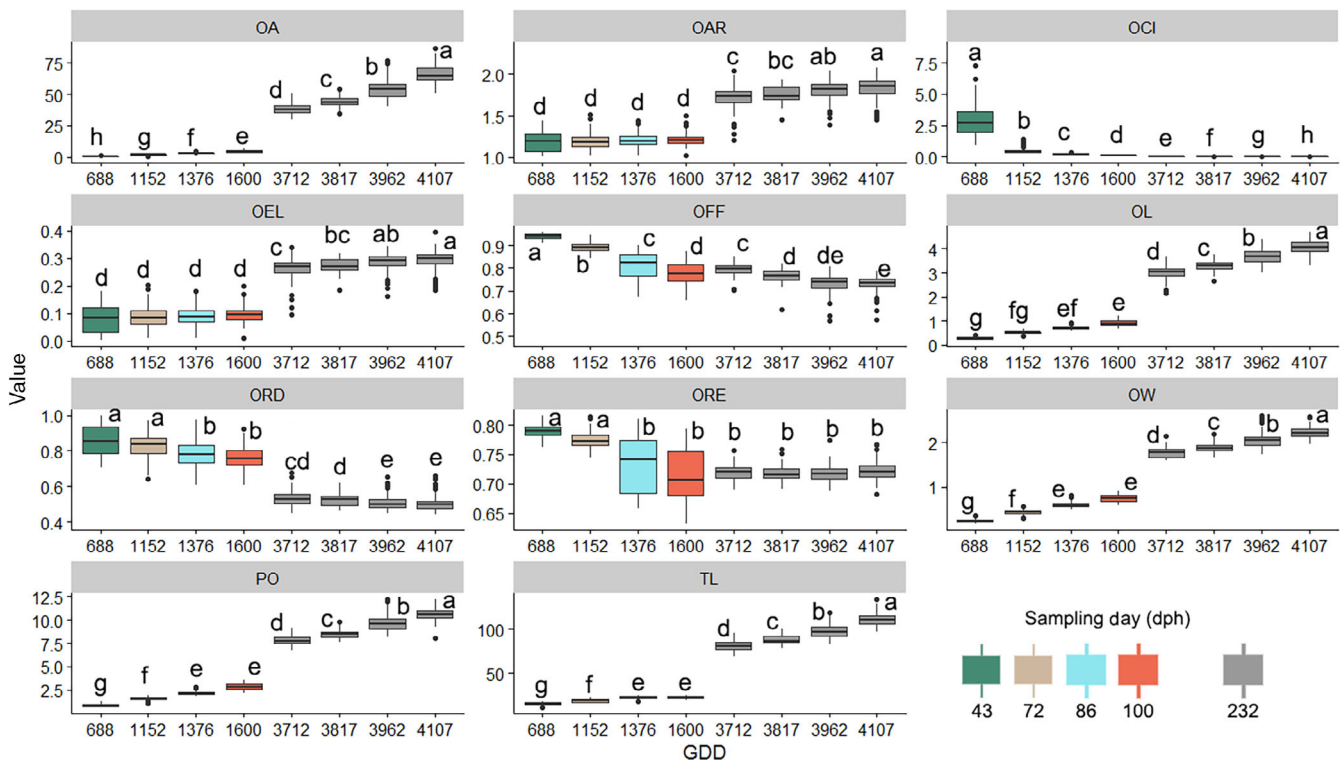

FIGURE 3 Otolith morphometric variables and fish total length (TL, mm) at growing degree-day (GDD, °C · day) of larvae and juvenile seabass reared at 16 and 21°C (color of boxplot indicates the sampling date). Different uppercase letters indicate significant differences ($p < 0.05$) between values of GDD.

variation in otolith contour of each individual and were thus used for further analysis. After PCA on the EFDs, only the first seven PCs were kept for the shape matrix according to the broken-stick model (which, in this case, corresponded to a threshold of 6.62% of the total variance explained). These six PCs explained 94.75% of the total variance

in the EFDs. The mixed-effects model detected no significant directional asymmetry differences between left and right otolith shape. The amplitude of directional asymmetry (DA), measured as the percentage of the nonoverlapping surface between the right and left otolith shapes throughout the experiment, was on average equal to

TABLE 1 Average percentage of nonoverlapping surface between the two reconstructed otolith shapes at the day of sampling and the growing degree-day level.

dph number (D)	GDD value (°C·day)	D 43 688°C·day	D 72 1152°C·day	D 86 1376°C·day	D 100 1600°C·day	D 232 3712°C·day	D 232 3817°C·day	D 232 3962°C·day	D 232 4107°C·day
D 43	688°C·day								
D 72	1152°C·day	7.20							
D 86	1376°C·day	10.28	3.48						
D 100	1600°C·day	13.86	6.90	5.17					
D 232	3712°C·day	26.87	21.34	20.52	18.20				
	3817°C·day	28.52	23.05	22.08	19.87	2.73			
	3962°C·day	30.58	25.26	24.27	21.88	5.48	2.48		
	4107°C·day	30.80	25.65	24.75	22.44	5.79	3.51	2.14	

1.33%. The amplitude of the DA increased from 43 to 100 dph to reach a value of 1.89% of nonoverlapping surface found in the dorso-posterior area (Figure 2).

After 100 dph, the observed DA according to the temperature treatment was around this value but by contrast characterized by the antero-posterior area (i.e., *rostrum* and *antirostrum* areas; Figure 2). Among the size parameters and shape indices, AO and OW showed significant differences between right and left otoliths at 43 dph ($p > 0.05$, mixed-effects models; Figure 3). During this life stage, many shape indexes showed a significant difference between the left and right ears (AO, LO, PO, ORD, ORE, and OFF; Figure 2).

From 43 to 100 dph, the growth of the otolith according to its length (OL), width (OW), and fish length (TL) had the same trend (Figure 3). However, the otolith growth was not the same in all directions and this was demonstrated by a change in otolith shape. OCI and OFF decreased significantly from 43 dph (i.e., GDD = 688°C·day) to 100 dph (i.e. GDD = 1600°C·day) (Figure 3).

Moreover, during this time, the average percentage of nonoverlapping surface between the two levels of GDD or time decreased regularly with the age of fish (Table 1). The evolution of normalized otolith shape from hatching to 100 dph (i.e., GDD = 1600°C·day) resulted in two main successive changes: a growth in the antero-posterior axis faster than that in the dorso-ventral axis, which changed the circular shape of the otolith at hatching, and an increasing complexity of the area between the rostrum and anti-rostrum (Figure 2).

3.2 | Temperature effect

During the first 100 days of this experiment, while the otolith growth and the fish growth are linked, ORE did not show a significant difference from 86 dph (i.e., GDD = 1376°C·day), which translated into relative stability of rectangularity expressed by the otolith shape. This temperature effect was observable between four normalized otolith shapes with this evolution, which followed the GDD value (Figure 4). Despite this, the difference between two reconstructed otolith shapes decreased with GDD value (Table S3). To model the somatic growth (i.e., the total length of the fish as the variable) and otolith shape (i.e. size parameters, shape indices, and EFDs as the variables), three tested multivariate mixed-effects models were applied to optimize the temperature effect (i.e., difference in the selected random effects) and the best-fitting model of the data was selected for each response variable (Table 2). As for fish growth, the selected model for many otolith shape descriptors did not integrate the variability due to rearing tanks and temperature treatments, which was not the case for the selected model for otolith shape described by the EFD. The GDD always had a significant effect on all otolith shape descriptors with the exception of rectangularity (ORE, $p = 0.57$; Table 2). Regarding the evolution of the morphometric variables during this second part of this experiment (i.e., from 100 to 232 dph), there was a significant modification between the otolith shape (Figure 4). The otolith morphogenesis was positively correlated to the level of growing degree-day but also
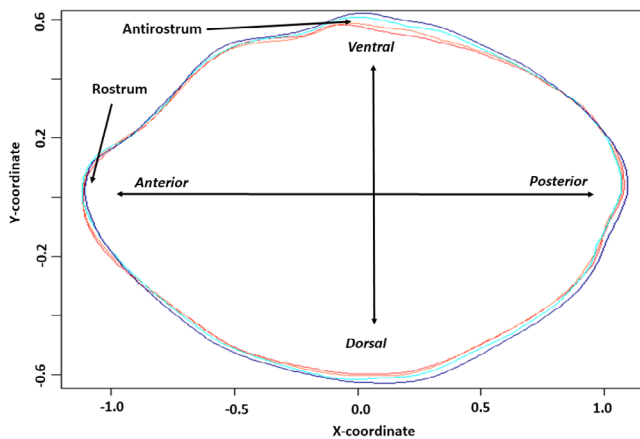
FIGURE 4 Comparison of otolith normalized shape at the end of the experiment (232 dph) for four temperature treatments: C1 (3712°C · day, dark blue line), C2 (3817°C · day, light blue line), C3 (3962°C · day, orange line), and C4 (4107°C · day, red line).

TABLE 2 Selected model and effect of growing degree-day (GDD) in each model by fish total length and otolith morphometric variables.

Selected model	GDD effect
$TL \sim \alpha_0 + \alpha_1 \cdot GDD$	$p < 0.05$
$OL \sim \alpha_0 + \alpha_1 \cdot GDD$	$p < 0.05$
$PO \sim \alpha_0 + \alpha_1 \cdot GDD$	$p < 0.05$
$OA \sim \alpha_0 + \alpha_1 \cdot GDD$	$p < 0.05$
$OW \sim \alpha_0 + \alpha_1 \cdot GDD$	$p < 0.05$
$OEL \sim \alpha_0 + \alpha_1 \cdot GDD$	$p < 0.05$
$ORD \sim \alpha_0 + \alpha_1 \cdot GDD$	$p < 0.05$
$OAR \sim \alpha_0 + \alpha_1 \cdot GDD$	$p < 0.05$
$OCI \sim (\alpha_0 + \mu_{0,C}) + \alpha_1 \cdot GDD$	$p < 0.05$
$ORE \sim (\alpha_0 + \mu_{0,C}) + \alpha_1 \cdot GDD$	$p = 0.57$
$OFF \sim (\alpha_0 + \mu_{0,C}) + \alpha_1 \cdot GDD$	$p < 0.05$
$PCs \sim (\alpha_0 + \mu_{0,R} + \mu_{0,C}) + (\alpha_1 + \mu_{1,R}) \cdot GDD$	$p < 0.05$

Abbreviations: OA, area; OL, length; ORE, OAR and rectangularity; OCI, ellipticity; OEL, aspect-ratio; OFF, form-factor; ORD, circularity; OW, width; PCs, principal components; PO, perimeter; TL, total length.

was dependent on the temperature level (Figure 4 and Table 2). In the same way, the results of otolith and fish lengths at 232 dph showed these lengths were also positively correlated to the level of growing degree-day (Figure 3).

4 | DISCUSSION

4.1 | Ontogenic effect

The growth mechanisms of otoliths and their morphogenesis during the early life stages of fish are known as biomineralization. This mechanism begins in the embryo with a complex of precursor particles (i.e., glycoproteins and glycogen, which eventually form the primordium) that are attached to the saccular epithelial tissue (Thomas & Swearer, 2019). These primordia control the direction of mineral precipitation (Jolivet et al., 2008). The otolith morphogenesis is controlled by the biomineralization process, which remains poorly understood (De Pontual et al., 2024). Recently, the three-dimensional spatial heterogeneity of the organic and inorganic compositions of the otolith was observed indeed with asymmetric of chemical composition between the proximal and distal sides of the otolith, which is species-dependent effect (De Pontual et al., 2024). However, the chemical element incorporation in the crystal lattice (i.e., calcium carbonate, $CaCO_3$) could be explained by these environmental concentrations and the physiological processes during early ontogeny (De Pontual et al., 2024; Hüssy et al., 2021; Loeppky et al., 2021; Thomas & Swearer, 2019). The shifts and the evolution of the otolith shape are linked to physiological mechanisms and environmental disturbance, especially of temperature and salinity (De Pontual et al., 2024; Geffen, 1987; Hüssy et al., 2021; Loeppky et al., 2021; Toole et al., 1993; Vignon, 2018). For flatfish species, the sagittal otoliths are circular, but after metamorphosis their shape becomes more complex with the formation of accessory growth centers (Lagardère &

Troadec, 1997; Modin et al., 1996; Sogard, 1991; Toole et al., 1993) and more precisely during settlement to be adapted to a bottom-living fish (Alhossaini et al., 1989; Karakiri et al., 1989; Okada et al., 2001). The development of secondary growth centers may be governed by changes in the direction of gravity during the shift from dorso-ventral to lateral swimming orientation (Ambrose et al., 1993; Toole et al., 1993). However, as for flatfish species, in gadoid species (round-fish species), sagittal otoliths were also subject to several morphological changes as fish transform from larvae to juveniles. The initial spherical form becomes elongated, with accessory growth centers and then a crenulated shape (Brown et al., 2001; Hüssy, 2008; Irgens et al., 2017; Radtke, 1989). Seabass larvae do not have a settlement period, as in flatfish and gadoid species along with the development of secondary growth centers, but their otoliths also undergo an important transformation. Otolith growth patterns are characterized by a negative allometric relationship between length and width (Simoneau et al., 2000). This study on seabass corroborated the studies on other fish species, indicating the first shift period with the elongation of otoliths which takes place prior to 70 dph. After this date, the otolith shape of seabass continues to become more complex, particularly at the area between the rostrum and anti-rostrum. This life stage is characterized from hatching by metamorphosis but also by the time of first feeding. The development during the early life stage is also linked to other factors such as food availability (including the match/mismatch hypothesis; Cushing, 1990) and predation pressure (e.g., the "bigger-is-better" mechanism) (Hare & Cowen, 1997).

Metamorphosis, in addition to having an effect on the otolith shape of fish, is the source of the shape asymmetry between the right and left otoliths because it causes a unique asymmetric body shape and a lateralized behavior from adaptation to a bottom-living lifestyle for flatfish (Okada et al., 2001). This involves relocation of the anterior

part of the frontal bones from the blind side to the ocular side (Brewster, 1987). This modification of body shape involves a gravity effect as a source of otolith asymmetry in flatfish (Schreiber, 2006). However, other factors could explain this significant directional symmetry, especially for roundfish species which have been studied, such as *Boops boops* (Mahé et al., 2018), *Liza ramada* (Rebaya et al., 2017), *Diplodus annularis* (Trojette et al., 2015), *Diplodus puntazzo* (Bostanci et al., 2016), *Clupea harengus* (Bird et al., 1986; Mille et al., 2015), *Merlangius merlangus* (Mille et al., 2015), and *Scomberomorus niphonius* (Zhang et al., 2016). The amplitude of directional asymmetry could be dependent on the sampled location and partly considered as a response to the environmental patterns (Mille et al., 2015). Our analysis showed that the amplitude of DA increased from 43 to 100 dph due to the dorso-posterior area (Figure 2). After 100 dph, the DA according to the temperature treatment was stabilized, without that this value of DA was not significant in seabass.

4.2 | Temperature effect

Temperature affects the growth of fish through direct effects (i.e., metabolism) and indirect effects (i.e., relationship with biotic factors as available food) (Paloheimo & Dickie, 1966; Uphoff et al., 2013). Fish experience higher growth rates when their metabolic activity rises with increasing temperature (Clarke & Johnston, 1999; IPCC, 2014). This relationship applies up to the thermal optimum of the species in question when food is available. During the early life stage of cod (*Gadus morhua*), among the factors affecting the formation and number of crenulations in the otolith outline, environmental factors, especially temperature and feeding level, have a greater influence than genetic difference (Cardinale et al., 2004; Hüssy, 2008; Irgens, 2018). A temperature effect during these early life stages has been demonstrated on otolith growth and shape. The experimental approach with several temperature treatments showed that calcite precipitation and consequently the growth rate of otolith increased with water temperature (Loeppky et al., 2021; Mahé et al., 2019). The temperature could be affected by the incorporation of chemical elements in the otolith having an impact on the shape and density (Loeppky et al., 2021). Our results on seabass corroborated the finding that temperature positively influenced fish and otolith growth. These studies have been carried out by comparing larvae or juveniles from different periods in situ or from different experimental temperature conditions in parallel (Hüssy, 2008; Loeppky et al., 2021; Mahé et al., 2019; Otterlei et al., 2002; Radtke, 1989; Stormer & Juanes, 2016). If temperature is a key factor affecting growth in fishes and their otoliths, resulting in mean temperature around the fish life positively influencing growth, the temperature range could also be a crucial component of the temperature effect, particularly where habitats change during migration (e.g., season, feeding, reproduction, settlement etc.). Adult and juvenile fish possess competent physiological processes that enable these organisms to acclimate to changing environmental conditions (Ishimatsu et al., 2008). However, early life stages are more vulnerable to environmental challenges because they

possess higher surface area to volume ratios and have not yet fully developed the homeostatic mechanisms present in adult fish (Hurst et al., 2013). Seabass, larvae, and juveniles develop in sheltered coastal areas or estuarine nurseries during the first year of life and then migrate (Kelley, 1988). Only one study on herring larvae analyzed the effect of changing temperatures on otolith growth and the increment deposition rate using an experimental approach (Folkvord et al., 2004). The relationship between otolith size and fish length of herring showed that otolith growth is more temperature-dependent than somatic growth (Folkvord et al., 2000; Folkvord et al., 2004). Our results on seabass show that both otolith and somatic growth are temperature dependent. A recent study on juvenile Australasian snapper (*Chrysophrys auratus*) reared in the laboratory, which was focused on metabolic effects on carbon isotopes in fish tissues, showed that the amount of $\delta^{13}C$ in otoliths, reflecting the proportional contributions of environmental water and diet, was linked to the temperature level (Martino et al., 2019). Consequently, the metabolic rate was directly proportional to the temperature level influence carbon incorporation for all tissues and the otolith. This partly explained the difference in otolith growth according to the experiment temperature. The experiment on herring larvae consisted of four temperature conditions (4°C, 12°C, and two others shifted two times with 4/8/4°C and 12/8/12°C) and showed that the size and width of the otolith daily increment were temperature-dependent (Folkvord et al., 2004). Another recent study on seabass larvae reared at 15 and 20°C concluded that otolith shape was influenced significantly by water temperature (Mahé et al., 2019). Likewise, our study showed that at 232 dph seabass otolith growth was correlated positively to growing degree-day. Moreover, for herring larvae, a significant temperature effect was observed on the otolith growth rate (slower growing fish having larger otoliths) (Folkvord et al., 2000). Our study, in the same way, identified seabass at 21°C as having the highest otolith growth and the highest otolith elongation (e.g., smaller ratio between width and length). Consequently, the temperature effect due to level and changing temperature had the same trend on the shape otolith for a small pelagic species (e.g., herring) and a demersal species (e.g., seabass). The otolith morphological difference in rockfishes species was explained by the geographical factor and especially the feeding habitat, which could be reflected fish adaptation to the sound and sensory environment (Gauldie & Crampton, 2002; Tuset et al., 2016). Moreover, deep-water and long-living species present larger, wider, and heavier otoliths than short-living species (Tuset et al., 2016). Our results on the otolith shape of seabass corroborated this hypothesis. To observe otolith morphogenesis, this study shows that among the commonly used descriptors (i.e., size parameters, shape indices, and EFDs), EFDs described the otolith outline better than the univariate descriptors. The indices are directly related to otolith size (size parameters) or proxies of otolith shape (shape indices). Consequently, the number of descriptors used in the analysis could be reduced. This difference between shape descriptors is explained by the detailed level of outline which is integrated into the descriptor. Conversely, the weight or volume of otolith could also be good proxies to characterize otolith shape because they integrate the growth in three dimensions

(Beyer & Szedlmayer, 2010). The effect of temperature on otolith shape is the sum of GDD and the relationship between GDD and tank temperature. In fact, otolith shape is significantly influenced by the sum of degree-days but the evolution speed is correlated positively to the tank temperature. Moreover, GDD is widely used to measure temperature and climate effects on the growth of vegetables and field crops (Neuheimer & Taggart, 2007; Trudgill et al., 2005). In fisheries science this approach could be used to analyze ontogenetic growth and its underlying factors (only 5% of temperature-related growth studies between 1980 and 2006 used the GDD value and not only dph number; Legg et al., 1998), but the GDD tool is starting to increase. The degree-day assumes the growth of fish or otoliths to be linear with and solely a function of temperature (Legg et al., 1998). However, there are temperature-independent regulators of fish growth (i.e., population density, genetic, food availability) which reduce the effect of temperature on fish growth. On the other hand, assuming temperature is the only contributor to growth allows to GDD to be uniquely account for temperature-dependent processes. Consequently, this index is more relevant than calendar time and temperature values (Uphoff et al., 2013). The length-at-age in 17 stocks of North Atlantic cod (*Gadus morhua*) was significantly correlated with GDD without correlation with calendar time (Neuheimer & Taggart, 2007). One recent study on seabass larvae reared at 15 and 20°C concluded that otolith shape was positively correlated to water temperature (Mahé et al., 2019). In our study, independently the date of changing temperature, otolith shape and growth were positively correlated the effect of rising temperature through the different values of GDD.

In conclusion, the growth and morphogenesis of otoliths during the early life stages of fish are due to an ontogenic effect but are also temperature-dependent. The temperature affected only the modification level of the initial otolith shape (e.g., the evolution speed) and did not influence the final otolith shape (e.g., development direction is the same whatever the GDD value). The effect of temperature according to the constant value or with shift during this period of fish life depends on the GDD value.

AUTHOR CONTRIBUTIONS

K.M. and B.E. designed the research. B.C. realized the experimental design. F.C. and M.O.B. carried out the experimental study. G.B.D realized the samplings and organized the image acquisition. K.M. and B.E. carried out the statistical analysis. All authors provided input for the results and discussion. K.M. wrote the paper. All authors provided critical comments and were involved in the writing of the manuscript. All authors accepted the final version of the manuscript.

ACKNOWLEDGMENTS

CONFLICT OF INTEREST STATEMENT

The authors declare that they have no competing interests.

ORCID

Kélig Mahé https://orcid.org/0000-0002-6506-211X

REFERENCES

Alhossaini, M., Liu, Q., & Pitcher, T. J. (1989). Otolith microstructures indicating growth and smortality among plaice, *Pleuronectes platessa* L., post-larval sub-cohorts. *Journal of Fish Biology*, 35, 81–90. https://doi.org/10.1111/j.1095-8649.1989.tb03048.x

Ambrose, J. J., Sass, S. L., & Davis, M. F. (1993). Early growth, behaviour and otolith development of the winter flounder *Pleuronectes americanus*. *US Fishery Bulletin*, 91, 65–75.

Auguie, B., & Antonov, A. (2017). Package 'gridExtra'. 2017. https://cran.r-project.org/web/packages/gridExtra/gridExtra.pdf.

Barrow, J., Ford, J., Day, R., & Morrongiello, J. (2017). Environmental drivers of growth and predicted effects of climate change on a commercially important fish, *Platycephalus laevigatus*. *Marine Ecology Progress Series*, 598, 201–212. https://doi.org/10.3354/meps12234

Bates, D., Maechler, M., & Bolker, B. (2011). lme4: Linear mixed-effects models using S4 classes. R package version 0.999375-42. http://CRAN.R-project.org/package=lme4.

Begg, G., & Brown, R. (2000). Stock identification of haddock *Melanogramus aeglefinus* on Georges Bank based on otolith shape analysis. *Transactions of the American Fisheries Society*, 129, 935–945. https://doi.org/10.1577/1548-8659(2000)129%3C0935:SIOHMA%3E2.3.CO;2

Beyer, S. G., & Szedlmayer, S. T. (2010). The use of otolith shape analysis for ageing juvenile red snapper, Lutjanus campechanus. *Environmental Biology of Fishes*, 89, 333–340. https://doi.org/10.1007/s10641-010-9684-z

Bird, J. L., Eppler, D. T., & Checkley, D. M. (1986). Comparisons of herring otoliths using Fourier series shape analysis. *Canadian Journal of Fisheries and Aquatic Sciences*, 43, 1228–1234. https://doi.org/10.1139/f86-152

Bonhomme, R. (2000). Bases and limits to using 'degree.day' units. *European Journal of Agronomy*, 13(1), 1–10. https://doi.org/10.1016/S1161-0301(00)00058-7

Bostanci, D., Yilmaz, M., Yedier, S., Kurucu, G., Kontas, S., Darçin, M., & Polat, N. (2016). Sagittal otolith morphology of sharpsnout seabream *Diplodus puntazzo* (Walbaum, 1792) in the Aegean Sea. *International Journal of Morphology*, 34, 484–488. https://doi.org/10.4067/S0717-95022016000200012

Brett, J. R. (1979). Environmental factors and growth. *Fish Physiology*, 8, 599–675.

Brewster, B. (1987). Eye migration and cranial development during flatfish metamorphosis: A reappraisal (Teleostei: Pleuronectiformes). *Journal of Fish Biology*, 31, 805–833. https://doi.org/10.1111/j.1095-8649.1987.tb05281.x

Brown, A. L., Busby, M. S., & Mier, K. L. (2001). Walleye pollock Theragra chalcogramma during transformation from the larval to juvenile stage: Otolith and osteological development. *Marine Biology*, 139, 845–851. https://doi.org/10.1007/s002270100641

Cardinale, M., Doering-Arjes, P., Kastowsky, M., & Mosegaard, H. (2004). Effects of sex, stock, and environment on the shape of known-age Atlantic cod (*Gadus morhua*) otoliths. *Canadian Journal of Fisheries and Aquatic Sciences*, 61, 158–167. https://doi.org/10.1139/f03-151

Casselman, J. M. (1983). Determination of age and growth. In A. H. Weatherley & H. S. Gill (Eds.), *The biology of fish growth* (pp. 209–242). Academic Press.

Clarke, A., & Johnston, N. M. (1999). Scaling of metabolic rate with body mass and temperature in teleost fish. *The Journal of Animal Ecology*, 68, 893–905. https://doi.org/10.1046/j.1365-2656.1999.00337.x

Cushing, D. H. (1990). Plankton production and year-class strength in fish populations: An update of the match/mismatch hypothesis. *Advances in Marine Biology*, 26, 249–293. https://doi.org/10.1016/S0065-2881(08)60202-3

De Pontual, H., MacKenzie, K. M., Tabouret, H., Daverat, F., Mahé, K., Pecheyran, C., & Hüssy, K. (2024). Heterogeneity of otolith chemical composition from two-dimensional mapping: Relationship with biomineralization mechanisms and implications for microchemistry analyses. *Journal of Fish Biology*, 104(1), 20–33. https://doi.org/10.1111/jfb.15561

Ferrari, S., Chatain, B., Cousin, X., Leguay, D., Vergnet, A., Vidal, M. O., Vandeputte, M., & Bégout, M. L. (2014). Early individual electronic identification of sea bass using RFID microtags: A first example of early phenotyping of sex-related growth. *Aquaculture*, 426-427, 165–171. https://doi.org/10.1016/j.aquaculture.2014.01.033

Folkvord, A., Blom, G., Johannessen, A., & Moksness, E. (2000). Growth dependent age estimation in herring (*Clupea harengus* L.) larvae. *Fisheries Research*, 46, 91–103. https://doi.org/10.1016/S0165-7836(00)00136-3

Folkvord, A., Johannessen, A., & Moksness, E. (2004). Temperature-dependent otolith growth in Norwegian spring-spawning herring (*Clupea harengus* L.) larvae. *Sarsia*, 89, 297–310. https://doi.org/10.1080/00364820410002532

Fossen, I., Albert, O. T., & Nilssen, E. M. (2003). Improving the precision of ageing assessments for long rough dab by using digitised pictures and otolith measurements. *Fisheries Research*, 60, 53–64. https://doi.org/10.1016/S0165-7836(02)00063-2

Fox, J., & Weisberg, S. (2011). *An R companion to applied regression* (2nd ed.). SAGE Publications.

Fulton, T. W. (2004). The rate of growth of fishes. 22nd Annual Report of the Fishery Board of Scotland. pp. 141-241.

Fusco, G., & Minelli, A. (2010). Phenotypic plasticity in development and evolution: Facts and concepts. Introduction. *Philosophical Transactions of the Royal Society B*, 365, 547–556. https://doi.org/10.1098/rstb.2009.0267

Gauldie, R. W., & Crampton, J. S. (2002). An eco-morphological explanation of individual variability in the shape of the fish otolith: Comparison of the otolith of *Hoplostethus atlanticus* with other species by depth. *Journal of Fish Biology*, 60, 1204–1221. https://doi.org/10.1111/j.1095-8649.2002.tb01715.x

Gauldie, R. W., & Nelson, D. G. A. (1990). Otolith growth in fishes. *Comparative Biochemistry and Physiology*, 97, 119–135. https://doi.org/10.1016/0300-9629(90)90159-P

Geffen, A. J. (1987). Methods of validating daily increment deposition in otoliths of larval fish. In R. C. Summerfelt & G. E. Hall (Eds.), *Age and growth of fish* (pp. 223–240). Iowa State University Press.

Hare, J. A., & Cowen, R. K. (1997). Size, growth, development, and survival of the planktonic larvae of *Pomatomus saltatrix* (Pisces: Pomatomidae). *Ecology*, 78, 2415–2431. https://www.jstor.org/stable/2265903

Hay, G., Richardson, A. J., & Robinson, C. (2005). Climate change and marine plankton. *Trends in Ecology & Evolution*, 20, 338–344. https://doi.org/10.1016/j.tree.2005.03.004

Hofmann, G. E., & Todgham, A. E. (2010). Living room in the now: Physiological mechanisms to tolerate has rapidly changing environment. *Annual Review of Physiology*, 72, 127–145. https://doi.org/10.1146/annurev-physiol-021909-135900

Hurst, T., Fernandez, E., & Mathis, J. (2013). Effects of ocean acidification on hatch size and larval growth of walleye pollock (*Theragra chalcogramma*), ICES. *Journal of Marine Science*, 70, 812–822. https://doi.org/10.1093/icesjms/fst053

Hüssy, K. (2008). Otolith shape in juvenile cod (*Gadus morhua*): Ontogenetic and environmental effects. *Journal of Experimental Marine Biology and Ecology*, 364, 35–41. https://doi.org/10.1016/j.jembe.2008.06.026

Hüssy, K., Limburg, K. E., de Pontual, H., Thomas, O. R. B., Cook, P. K., Heimbrand, Y., Blass, M., & Sturrock, A. M. (2021). Trace element patterns in otoliths: The role of biomineralization. *Reviews in Fisheries Science & Aquaculture*, 29, 445–477. https://doi.org/10.1080/23308249.2020.1760204

IPCC. (2014). Climate change 2014: Synthesis report. Contribution of Working Groups I, II and III to the Fifth Assessment Report of the Intergovernmental Panel on Climate Change, IPCC. http://hdl.handle.net/10013/epic.45156

Irgens, C. (2018). Otolith structure as indicator of key life history events in Atlantic cod (*Gadus morhua*). M.Sc. Thesis, the University of Bergen. http://bora.uib.no/handle/1956/18712

Irgens, C., Kjesbu, O. S., & Folkvord, A. (2017). Ontogenetic development of otolith shape during settlement of juvenile Barents Sea cod (*Gadus morhua*). *ICES Journal of Marine Science*, 74, 2389–2397. https://doi.org/10.1093/icesjms/fsx088

Ishimatsu, A., Hayashi, M., & Kikkawa, T. (2008). Fishes in high-CO_2, acidified oceans. *Marine Ecology Progress Series*, 373, 295–302. https://doi.org/10.3354/meps07823

Jolivet, A., Bardeau, J. F., Fablet, R., Paulet, Y. M., & De Pontual, H. (2008). Understanding otolith biomineralization processes: New insights into microscale spatial distribution of organic and mineral fractions from Raman microspectrometry. *Analytical and Bioanalytical Chemistry*, 392, 551–560. https://doi.org/10.1007/s00216-008-2273-8

Karakiri, M., Berghahn, R., & von Westernhagen, H. (1989). Growth differences in 0-group plaice Pleuronectes platessa as revealed by otolith microstructure analysis. *Marine Ecology Progress Series*, 55, 15–22. https://www.jstor.org/stable/24835060

Kelley, D. F. (1988). The importance of estuaries for sea bass, *Dicentrarchus labrax* (L.). *Journal of Fish Biology*, 33, 25–33. https://doi.org/10.1111/j.1095-8649.1988.tb05555.x

Kuhl, F., & Giardina, C. (1982). Elliptic Fourier features of a closed contour. *Computer Graphics and Image Processing*, 18, 236–258. https://doi.org/10.1016/0146-664X(82)90034-X

Lagardère, F., & Troadec, H. (1997). Age estimation in common sole *Solea solea* larvae: Validation of daily increments and evaluation of a pattern recognition technique. *Marine Ecology Progress Series*, 155, 223–237. https://www.jstor.org/stable/24858187

Legendre, P., & Legendre, L. F. J. (1998). *Numerical Ecology* (2nd ed.). Elsevier Science.

Legg, D., Strutimann, J., van Vleet, S., & Lloyd, J. (1998). Bias and variability in lower developmental thresholds estimated from field studies. *Journal of Economic Entomology*, 91(4), 891–898. https://doi.org/10.1093/jee/91.4.891

Lestrel, P. E. (2008). *Fourier descriptors and their applications in biology*. Cambridge University Press.

Loeppky, A. R., Belding, L. D., Quijada-Rodriguez, A. R., Morgan, J. D., Pracheil, B. M., Chakoumakos, B. C., & Anderson, W. G. (2021). Influence of ontogenetic development, temperature, and pCO_2 on otolith calcium carbonate polymorph composition in sturgeons. *Scientific Reports*, 11, 13878. https://doi.org/10.1038/s41598-021-93197-6

Mahé, K., Aumond, Y., Rabhi, K., Ellebode, R., Bellamy, E., Huet, J., Gault, M., & Roos, D. (2017). Relationship between somatic growth and otolith growth: A case study of the ornate jobfish *Pristipomoides argyrogrammicus* from the coast of Réunion (SW Indian Ocean). *African Journal of Marine Science*, 39(2), 145–151. https://doi.org/10.2989/1814232X.2017.1327886

Mahé, K., Gourtay, C., Bled Defruit, G., Chantre, C., de Pontual, H., Amara, R., Claireaux, G., Audet, C., Zambonino-Infante, J. L., & Ernande, B. (2019). Do environmental conditions (temperature and food composition) affect otolith shape during fish early-juvenile phase? An experimental approach applied to European seabass (*Dicentrarchus labrax*). *Journal of Experimental Marine Biology and Ecology*, 521, 151239. https://doi.org/10.1016/j.jembe.2019.151239

Mahé, K., Ider, D., Massaro, A., Hamed, O., Jurado-Ruzafa, A., Gonçalves, P., Anastasopoulou, A., Jadaud, A., Mytilineou, C., Elleboode, R., Ramdane, Z., Bacha, M., Amara, R., de Pontual, H., & Ernande, B. (2018). Directional bilateral asymmetry in otolith morphology may affect fish stock discrimination based on otolith shape analysis. *ICES Journal of Marine Science*, 76(1), 232–243. https://doi.org/10.1093/icesjms/fsy163

Martino, J. C., Fowler, A. J., Doubleday, Z. A., Grammer, G. L., & Gillanders, B. M. (2019). Using otolith chronologies to understand long-term trends and extrinsic drivers of growth in fisheries. *Ecosphere*, 10(1), e02553. https://doi.org/10.1002/ecs2.2553

McDonald, J. H. (2014). *Handbook of biological statistics* (1st ed.). Sparky House Publishing.

Mieszkowska, N., Kendall, M. A., Hawkins, S. J., Leaper, R., Williamson, P., Hadrman-Mountford, N. J., & Southward, A. J. (2006). Changes in the range of some common rocky shore species in Britain - a response to climate change? *Hydrobiologia*, 555, 241–251. https://doi.org/10.1007/1-4020-4697-9_20

Mille, T., Mahé, K., Villanueva, C. M., De Pontual, H., & Ernande, B. (2015). Sagittal otolith morphogenesis asymmetry in marine fishes. *Journal of Fish Biology*, 87, 646–663. https://doi.org/10.1111/jfb.12746

Modin, J., Fagerholm, B., Gunnarsson, B., & Pihl, L. (1996). Changes in otolith microstructure at metamorphosis of plaice, *Pleuronectes platessa* L. *ICES Journal of Marine Science*, 53, 745–748. https://doi.org/10.1006/jmsc.1996.0094

Morrongiello, J. R., & Thresher, R. E. (2015). A statistical framework to explore ontogenetic growth variation among individuals and populations: A marine fish example. *Ecological Monographs*, 85, 93–115. https://doi.org/10.1890/13-2355.1

Neuheimer, A. B., & Taggart, C. T. (2007). The growing degree-day and fish size-at-age: The overlooked metric. *Canadian Journal of Fisheries and Aquatic Sciences*, 64(2), 375–385. https://doi.org/10.1139/f07-003

Neuheimer, A. B., Thresher, R. E., Lyle, J. M., & Semmens, J. M. (2011). Tolerance limit for fish growth exceeded by warming waters. *Nature Climate Change*, 1, 110–113. https://doi.org/10.1038/nclimate1084

Okada, N., Takagi, Y., Seikai, T., Tanaka, M., & Tagawa, M. (2001). Asymmetrical development of bones and soft tissues during eye migration of metamorphosing Japanese flunder *Paralichthys Olivaceus*. *Cell and Tissue Research*, 304, 59–66. https://doi.org/10.1007/s004410100353

Otterlei, E., Folkvord, A., & Nyhammer, G. (2002). Temperature dependent otolith growth of larval and early juvenile Atlantic cod (*Gadus morhua*). *ICES Journal of Marine Science*, 59, 401–410. https://doi.org/10.1006/jmsc.2001.1300

Paloheimo, J. E., & Dickie, L. M. (1966). Food and growth of fishes. II. Effects of food and temperature on the relation between metabolism and body weight. *Journal of the Fisheries Research Board of Canada*, 23, 869–908. https://doi.org/10.1139/f66-077

Pinheiro, J., Bates, D., DebRoy, S., & Sarkar, D. (2016). nlme: Linear and Nonlinear Mixed Effects 528 Models. R package version 3.1-128. https://cran.r-project.org/web/packages/nlme/nlme.pdf

Pörtner, H. O., & Knust, R. (2007). Climate change affects marine fishes through the oxygen limitation of thermal tolerance. *Science*, 315, 95–97. https://doi.org/10.1126/science.1135471

Price, T. D., Qvarnström, A., & Irwin, D. E. (2003). The role of phenotypic plasticity in driving genetic evolution. *Proceedings of the Royal Society of London – Series B: Biological Sciences*, 270, 1433–1440. https://doi.org/10.1098/rspb.2003.2372

Radtke, R. L. (1989). Larval fish age, growth, and body shrinkage: Information available from otoliths. *Canadian Journal of Fisheries and Aquatic Sciences*, 46, 1884–1894. https://doi.org/10.1139/f89-237

Réaumur, R. A. (1735). Observations du thermomètre faites pendant l'annee MDCCXXXV comparées à celles qui ont été faites sous la ligne à l'Isle-de-France, à Alger et en quelques-unes de nos Isles de l'Amerique. *Mémoires de l'Academie Royale des Sciences*, 1738, 545–576.

Rebaya, M., Ben Faleh, R., Khedher, M., Trojette, M., Marsaoui, B., Fatnassi, M., Chalh, A., Quignard, J.-P., & Trabelsi, M. (2017). Otolith shape discrimination of *Liza ramada* (Actinopterygii: Mugiliformes: Mugilidae) from marine and estuarine populations in Tunisia. *Acta Ichthyologica et Piscatoria*, 47(1), 13–21. https://doi.org/10.3750/AIEP/02006

Schreiber, A. M. (2006). Asymmetric craniofacial remodeling and lateralized behavior in larval flatfish. *The Journal of Experimental Biology*, 209, 610–621. https://doi.org/10.1242/jeb.02056

Simoneau, M., Casselman, J. M., & Fortin, R. (2000). Determining the effect of negative allometry (length/height relationship) on variation in otolith shape in lake trout (*Salvelinus namaycush*), using Fourier-series analysis. *Canadian Journal of Zoology*, 78, 1597–1603. https://doi.org/10.1139/z00-093

Smith, M. K. (1992). Regional differences in otolith morphology of the deep slope red snappers *Etelis carbunculus*. *Canadian Journal of Fisheries and Aquatic Sciences*, 49, 795–804. https://doi.org/10.1139/f92-090

Smoliński, S., & Mirny, Z. (2017). Otolith biochronology as an indicator of marine fish responses to hydroclimatic conditions and ecosystem regime shifts. *Ecological Indicators*, 79, 286–294. https://doi.org/10.1016/j.ecolind.2017.04.028

Sogard, S. M. (1991). Interpretation of otolith microstructure in juvenile winter flounder (*Pseudopleuronectes americanus*): Ontogenetic development, daily increment validation and somatic growth relationships. *Canadian Journal of Fisheries and Aquatic Sciences*, 48(10), 1862–1871. https://doi.org/10.1139/f91-220

Stormer, D. G., & Juanes, F. (2016). Effects of temperature and ration on the otolith-to-somatic size relationship in juvenile Chinook salmon (*Oncorhynchus tshawytscha*): A test of the direct proportionality assumption. *Marine and Freshwater Research*, 67, 913–924. https://doi.org/10.1071/MF15206

Thomas, C., Cameron, A., Green, R., Bakkenes, M., Beaumont, L. J., Yvonne, C., Erasmus, B. F., De Siqueira, M. F., Grainger, A., Hannah, L., Hughes, L., Huntley, B., Van Jaarsveld, A. S., Midgley, G. F., Miles, L., Ortega-Huerta, M. A., Peterson, A. T., Phillips, O. L., & Williams, S. E. (2004). Extinction risk from climate change. *Nature*, 427, 145–148. https://doi.org/10.1038/nature02121

Thomas, O. R. B., & Swearer, S. E. (2019). Otolith biochemistry-a review. *Reviews in Fisheries Science & Aquaculture*, 27, 458–489. https://doi.org/10.1080/23308249.2019.1627285

Toole, C. L., Markle, D. F., & Harris, P. M. (1993). Relationships between otolith microstructure, microchemistry, and early life history events in Dover sole, *Microstomus pacificus*. *US Fishery Bulletin*, 91, 732–753.

Trojette, M., Ben Faleh, R., Fatnassi, M., Marsaoui, B., Mahouachi, N. E. H., Chalh, A., Chalh, A., Quignard, J.-P., & Trabels, M. (2015). Stock discrimination of two insular populations of *Diplodus annularis* (Actinopterygii: Perciformes: Sparidae) along the coast of Tunisia by analysis of otolith shape. *Acta Ichthyologica et Piscatoria*, 45, 363–372. https://doi.org/10.3750/AIP2015.45.4.04

Trudgill, D. L., Honek, A., Li, D., & van Straalen, N. M. (2005). Thermal time – Concepts and utility. *The Annals of Applied Biology*, 146(1), 1–14. https://doi.org/10.1111/j.1744-7348.2005.04088.x

Tuset, V. M., Otero-Ferrer, J. L., Gómez-Zurita, J. G., & Venerus, L. (2016). Otolith shape lends support to the sensory drive hypothesis in rockfishes. *Journal of Evolutionary Biology*, 29, 2083–2097. https://doi.org/10.1111/jeb.12932

Uphoff, C. S., Schoenebeck, C. W., Wyatt Hoback, W., Koupal, K. D., & Pope, K. L. (2013). Degree-day accumulation influences annual variability in growth of age-0 walleye (2013). *Fisheries Research*, 147, 394–398. https://doi.org/10.1016/j.fishres.2013.05.010

Venables, W. N., & Ripley, B. D. (2002). *Modern applied statistics with S* (4th ed.). Springer.

Vignon, M. (2018). Short-term stress for long-lasting otolith morphology – Brief embryological stress disturbance can reorient otolith ontogenetic trajectory. *Canadian Journal of Fisheries and Aquatic Sciences*, *75*(10), 1713–1722. https://doi.org/10.1139/cjfas-2017-0110

Weisberg, S., Spangler, G., & Richmond, L. S. (2010). Mixed effects models for fish growth. *Canadian Journal of Fisheries and Aquatic Sciences*, *67*, 269–277. https://doi.org/10.1139/F09-181

Wickham, H. (2016). *ggplot2: Elegant graphics for data analysis*. Springer-Verlag.

Zhang, C., Ye, Z., Li, Z., Wan, R., Ren, Y., & Dou, S. (2016). Population structure of Japanese Spanish mackerel *Scomberomorus niphonius* in the Bohai Sea, the Yellow Sea and the East China Sea: Evidence from random forests based on otolith features. *Fisheries Science*, *82*, 251–256. https://doi.org/10.1007/s12562-016-0968-x

SUPPORTING INFORMATION

Additional supporting information can be found online in the Supporting Information section at the end of this article.